The initial stages of Case II diffusion at low penetrant activities

Ronald C. Lasky and Edward J. Kramer
Department of Materials Science and Engineering and the Materials Science Center, Cornell University, Ithaca, NY 14853, USA

and C.-Y. Hui*
Department of Theoretical and Applied Mechanics and the Materials Science Center, Cornell University, Ithaca, NY 14853, USA
(Received 4 August 1987; revised 16 September 1987; accepted 25 September 1987)

Rutherford backscattering spectrometry (R BS) has been used to measure the volume fraction *versus* depth profiles of iodohexane vapour diffusing into glassy polystyrene. At penetrant activities of less than 0.40 the surface concentration increases slowly and approaches equilibrium only after very long vapour exposures. Since Case II diffusion is observed to begin only after a critical concentration of penetrant is reached, these kinetics create an induction time for the Case II process. However, the swelling kinetics of the surface are still slow after the induction time has elapsed even though the diffusion coefficient behind the front is much larger than that in the polymer ahead of the front. The agreement between these swelling kinetics and those predicted by the model of Thomas and Windle is relatively poor. On the other hand, if the Thomas and Windle model is modified (1) to allow the viscosity of the polymer to decrease exponentially with osmotic pressure, with the decrease set to match that observed in separate creep measurements as a function of tensile stress, and (2) to include an initial volume fraction of rapidly filling interstitial sites, which we take to be due to the initial free volume, the agreement between the model and the experiment is much better.

(Keywords: Case II diffusion; surface swelling; induction time; Rutherford backscattering spectrometry)

INTRODUCTION

Although Case II diffusion has been seriously studied since Scott's work on ebonite[1], only in recent years have models been created that faithfully predict its three central aspects[2-7]. These characteristics, first pointed out by Alfrey[8], are:

1 A sharp advancing boundary separates an inner glassy core from an outer swollen and rubbery shell.

2 The swollen gel behind the advancing penetrant front is almost in equilibrium.

3 The boundary between the swollen gel and glassy core advances at a constant velocity.

It is possible with optical[4] and gravimetric[9-12] experiments to verify these conditions in a polymer/penetrant system.

The existence of an induction time is a fourth characteristic of Case II diffusion that has not received attention until recently[7]. Usually neither optical nor gravimetric techniques have the sensitivity needed to observe this feature, hence this oversight is not surprising. The application of Rutherford backscattering spectrometry (R BS) to Case II diffusion makes it possible to investigate the details of this induction time and obtain new information on the initial stages of Case II diffusion.

THEORETICAL DEVELOPMENT

The Thomas and Windle model of Case II diffusion

Of all the theories, that of Thomas and Windle[2-7] appears most faithfully to predict all of the characteristics of Case II diffusion. Their model assumes that as the penetrant diffuses into the polymer it creates a thermodynamic (osmotic) pressure. This osmotic pressure, in turn, creates the 'sites' for more penetrant. Since this site creation cannot occur instantaneously an induction time is predicted. Thomas and Windle (TW) developed and numerically solved the equations describing this model[2]. Recent work[13,14] has emphasized improving the mathematical foundations and computational convenience of the TW model but as yet no comprehensive test of the model *versus* experiment has been reported. The experiments reported here represent the first step in such testing. In preparation for the comparison with experiment to follow, we first briefly review the salient features of the TW model.

The TW model can be considered to be a coupling of an osmotic-pressure-driven viscous response of the polymer (polymer chain relaxation) and Fickian diffusion. This osmotic pressure is approximated by[13]

$$P=(k_BT/\Omega)\ln(\phi_e/\phi) \quad (1)$$

where k_B is the Boltzmann constant, Ω is the penetrant partial molecular volume, ϕ_e is the penetrant volume fraction in equilibrium and ϕ is the penetrant volume fraction. The polymer chain relaxation is approximated by the linear viscous relationship

$$\partial\phi/\partial t=P/\eta \quad (2)$$

where the viscosity, η, is given by

$$\eta=\eta_0\exp(-m\phi) \quad (3)$$

where m and η_0 are material constants.

* To whom correspondence should be addressed

0032-3861/88/040673-07$03.00

It is more accurate, and only slightly more complicated, to represent the osmotic pressure as the logarithm of the ratio of activities[2]. Hence

$$P=(k_BT/\Omega)\ln(a_e/a) \quad (4)$$

where a_e is the activity of the penetrant in equilibrium and a is the activity of the penetrant. To obtain an expression for a in terms of ϕ, or a_e in terms of ϕ_e, let us consider a polymer/penetrant mixture in equilibrium with the penetrant vapour. By applying the Flory–Huggins theory for solvent/polymer mixtures, we find the penetrant activity in the polymer and surrounding vapour is[15]

$$a=\phi\exp(1-\phi)\exp\{\chi_1(1-\phi)^2\} \quad (5a)$$

where χ_1 is the polymer/solvent interaction parameter. If the solvent is a 'good' solvent for the polymer, χ_1 is nearly equal to zero. In this case equation (5a) reduces to

$$a=\phi\exp(1-\phi) \quad (5b)$$

Guggenheim has shown that the solvent activity in many polymer/solvent systems can be approximated by equation (5b)[16].

The error in describing pressure by equation (1) instead of equation (4) can be greater than 30% for $\phi_e>0.6$. This paper will focus on solving the swelling equation numerically and so the more accurate representation of osmotic pressure will be used.

Surface swelling kinetics

Consider an experiment where a polymer sample is exposed to a penetrant vapour. *Figure 1* is a schematic of the apparatus used to perform such an experiment. The activity in the vapour is controlled by a mixture of polymer and solvent at the bottom of an Erlenmeyer flask. The volume fraction of solvent in this mixture is designated as ϕ_e since it will be the volume fraction in the polymer sample at equilibrium. The value of the vapour activity can then be determined by using equation (5b).

Equations (2), (3), (4) and (5b) describe the surface swelling kinetics in the above experiment. Combining these four equations results in the following relation for the osmotic-pressure-driven swelling rate of the polymer:

$$\partial\phi/\partial t=B\exp(m\phi)\ln\Theta \quad (6)$$

where

$$B=k_BT/\Omega\eta_0 \quad (7)$$

and

$$\Phi=a_e/a=\phi_e\exp(1-\phi_e)/\phi\exp(1-\phi) \quad (8)$$

Solving equation (6) for t we find

$$t=(1/B)\int_{\phi_i}^{\phi_f}\exp(-m\phi)/(\ln\Theta)\,d\phi \quad (9)$$

where ϕ_i is the initial penetrant volume fraction, and ϕ_f is the final penetrant volume fraction. The value of ϕ_i was assumed to be equal to zero in earlier work[2,13]. This assumption does not seem reasonable as there is probably some 'free volume' that the penetrant can occupy without polymer chain relaxation. As a starting point, however, we will begin with this value.

Equation (9) indicates that, contrary to the assumption used in applying Fick's laws, the surface volume fraction of penetrant does not immediately reach its equilibrium value. Time is needed to create sites for the penetrant. This penetrant site creation is the fundamental reason for the induction time in Case II diffusion.

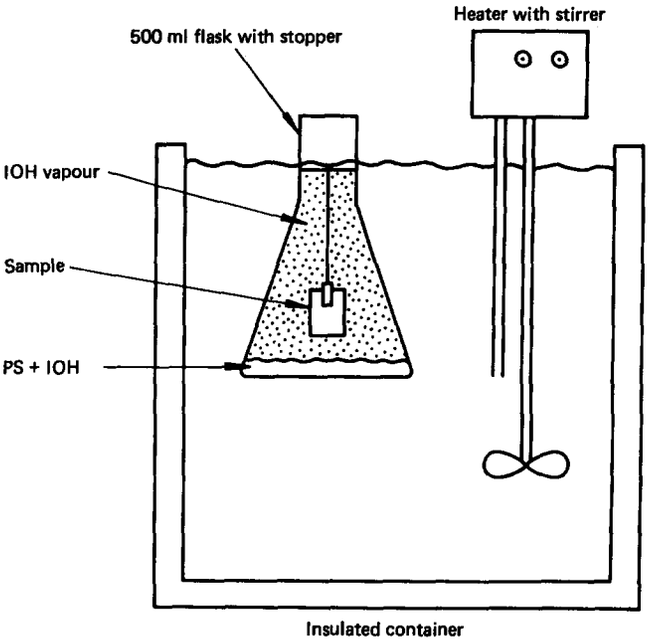

Figure 1 Schematic of the experimental apparatus used to expose the polystyrene samples to a controlled-activity iodohexane vapour

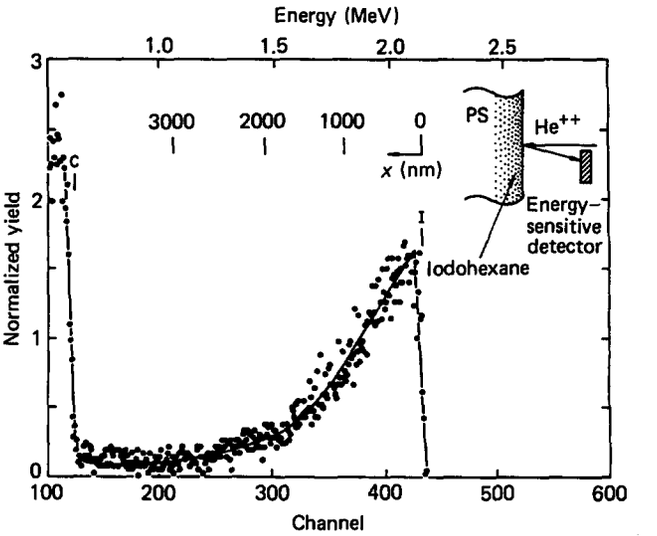

Figure 2 An RBS spectrum of iodohexane diffusing into polystyrene

EXPERIMENTAL PROCEDURE

Fundamentals of Rutherford backscattering spectrometry

A typical geometry for Rutherford backscattering spectrometry is shown in the insert to *Figure 2*. A He^{++} ion beam is incident on the sample. Some of these ions backscattered by nuclei at and below the polymer surface are collected by an energy-sensitive detector. The output of this detector is fed into a multichannel analyser, which

displays the number of ions *versus* ion energy. Analysis of this Rutherford backscattering spectrum yields elemental composition information as a function of depth up to a limiting depth of several micrometres for polymer samples.

The elemental composition information results from the influence of the mass of the target nucleus on the energy of the scattered He^{++} ion. From conservation of energy and momentum[17], the energy E of a He^{++} ion of mass m backscattered through an angle of 180° by a nucleus of mass M at the surface will be

$$E = KE_0 \tag{10}$$

where E_0 is the energy of the incident beam, and the kinematic factor K is

$$K = \{(M-m)/(m+M)\}^2 \tag{11}$$

The kinematic factor enables one to calculate the energy of the backscattered He^{++} ions but gives no information on the quantity of ions that are backscattered. This information is contained in the Rutherford scattering cross section, for a good approximation is[17]

$$\sigma = (e^2zZ/4E_0)^2\{\sin^{-4}(\theta/2) - 2(m/M)^2\} \tag{12}$$

where z and Z are the atomic numbers of the He^{++} ion and target respectively, e is the charge on the electron and θ is the angle between the incident and scattered beam. The total number of detected particles can then be obtained by integrating σ over the detector solid angle and multiplying by the number of incident particles and the number of target atoms per unit area.

When scattering occurs below the target surface the He^{++} ions lose energy due to inelastic collisions with electrons as they penetrate the sample. This energy loss may be calculated from the stopping cross section of the target ε_s defined by[17]

$$\varepsilon_s(E) = (N^{-1})dE/dx \tag{13a}$$

where N is the atomic density of the target. The values of $\varepsilon_s(E)$ are tabulated for pure elements but not for molecules such as polystyrene[18]. Bragg's rule can be used to estimate the stopping cross section for such molecules[17]. This rule states that the stopping cross section of the molecule is the weighted sum of the cross sections of the individual atoms, e.g. for polystyrene

$$\varepsilon_s C_8H_8 = 8\varepsilon_{sC} + 8\varepsilon_{sH} \tag{13b}$$

Using equations (13a) and (13b) it is possible to calculate an elemental depth scale in an inhomogeneous target. The details of these computations have appeared in the literature[17-22].

Selecting a suitable polymer/penetrant system for investigating the Case II diffusion mechanism with RBS requires several considerations. Obviously a polymer/-penetrant diffusion system must be chosen that exhibits this diffusion mode. Other considerations are that the penetrant should have a 'tag' nucleus with a large atomic mass and that the polymer should contain no heavy nuclei and be relatively immune from mass loss by ion radiation damage. Polystyrene which has only carbon and hydrogen is a good choice for the polymer, and a good candidate for the tag is iodine. The kinematic factor for a He^{++} ion backscattered from an iodine nucleus is 0.8814 while that for carbon is 0.2501. This large energy difference will allow a depth analysis of the iodine to $\sim 4\,\mu m$ below the surface (at 2.4 MeV) before the RBS signal from the deepest iodine nucleus overlaps that of the carbon at the polymer surface. The high Z of iodine also means that it can be detected at quite low levels (approximately 20 atomic ppm) due to its high value of σ. Since, for example, iodine ($Z = 53$) has a scattering cross section approximately ten times that of chlorine ($Z = 17$), iodine can be detected at concentrations about one tenth those of chlorine.

The polymer/penetrant system polystyrene/1-iodo-n-hexane (PS/IOH) has all of the above advantages. *Figure 2* is an RBS spectrum of iodohexane diffusing into polystyrene. The abscissa is the energy of the backscattered He^{++} ions (also read as channel number), while the ordinate is the normalized yield. The normalized yield is defined as $n/(Qe_{ch}\omega)$, where n is the number of backscattered ions collected in each channel, Q is the total charge hitting the sample, e_{ch} is the energy width of each channel (4.95 keV in this case) and ω is the detector solid angle (3.4 msr). The energies of the He^{++} ions backscattered from the carbon and iodine at the polymer surface are labelled on the figure. Helium ions scattered below the surface are recorded at lower energies. The depth scale on this figure was obtained by employing a computer algorithm developed by Doolittle[20,21] that uses equations (10)–(13). The depth scale indicates that it is possible to measure penetrant penetration to a depth of approximately 4 μm before the backscattering from the iodine begins to overlap with the backscattering from the carbon at the surface. A second algorithm due to Doolittle[20,21] can be used to convert the normalized yield data to the atomic fraction of iodine, from which the number of penetrant molecules per mer unit of the PS could be computed. The IOH volume fraction ϕ was computed from these data by assuming that the partial molar volumes of the components are equal to the molar volumes of the pure components. This algorithm was used to produce *Figure 3*, which is a penetrant volume

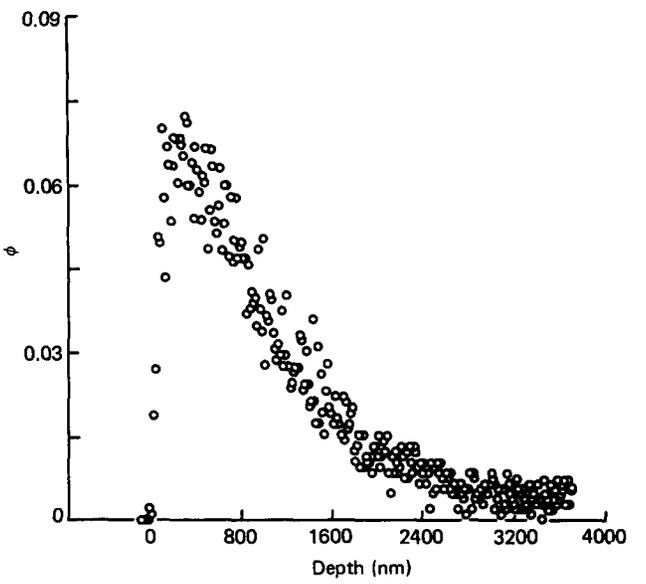

Figure 3 A penetrant volume fraction *versus* depth profile of iodohexane in polystyrene from the data in *Figure 2*

fraction *versus* depth profile corresponding to the RBS spectrum in *Figure 2.*

Sample preparation

Aluminium substrates 1.25 cm × 1.25 cm × 1 mm thick were metallurgically polished, etched in a 20% NaOH aqueous solution* and dip-coated in an 11% solution of polystyrene in toluene. The polystyrene had a molecular weight of 390 000 and a polydispersity index less than 1.10, as specified by the supplier, Pressure Chemical Co. The resulting films were dried in air for 24 h and were approximately 4 μm thick. The samples were subsequently annealed at 125°C for 1 h and physically aged at 50°C for 24 h. Controlled physical ageing was found to be necessary to produce a stable glass structure[23] in order to observe reproducible diffusion results. Ageing at 50°C was done to minimize the effects of ageing at room temperature after sample preparation[24].

Exposure of the PS to the IOH vapour was accomplished with the temperature-controlled water bath apparatus shown in *Figure 1.* The activity of the IOH was controlled by mixing known quantities of PS and IOH in the bottom of the flask and allowing the partial vapour pressure of the IOH in the flask to come to equilibrium. The ϕ_e of these mixtures ranged from 0.083 to 0.6. After exposure to the IOH vapour the samples were quickly immersed in liquid nitrogen since the diffusion could be very rapid at room temperature. The samples were transferred to the liquid-nitrogen-cooled stage of the RBS apparatus under a dry nitrogen atmosphere in a glove bag to minimize water condensation on the sample surface. All analyses were performed at a temperature below 100 K. Besides stopping further diffusion, the low temperature had the advantage of preventing mass loss and penetrant redistribution due to radiation damage in the polymer caused by the energetic He^{++} ions.

The absence of radiation damage effects on the IOH diffusion profile at these low temperatures was verified by collecting backscattering spectra after several different ion doses. Over a dose range from 20 to 2000 $\mu C\,cm^{-2}$ there was no effect on the resulting IOH volume fraction profiles, in accord with similar observations for polymethylmethacrylate-based photoresist and in polyimide[22,25].

RESULTS AND DISCUSSION

Diffusion profiles and the induction time

Figure 4 contains a series of penetrant volume fraction *versus* depth profiles from the PS film after various times of exposure to IOH vapour*. The IOH vapour had an activity $a_e = 0.19$ corresponding to an equilibrium IOH volume fraction in PS of $\phi_e = 0.083$. *Figure 5* shows a similar series of diffusion profiles after exposure to IOH vapour with $a_e = 0.37$, corresponding to $\phi_e = 0.16$. These figures indicate that at $\phi_e = 0.083$ Case II diffusion has not started in times greater than 10^6 s, whereas it starts after approximately 5×10^5 s at $\phi_e = 0.16$. In *Figure 5* the profile at 4.1×10^5 s indicates that Case II diffusion has just started at this time. This profile shows $\phi \approx 0.1$ at the surface and therefore it appears that this level of penetrant volume fraction at the surface is a requirement for Case II diffusion to begin. This observation suggests that at $\phi_e = 0.083$ Case II diffusion will never exist.

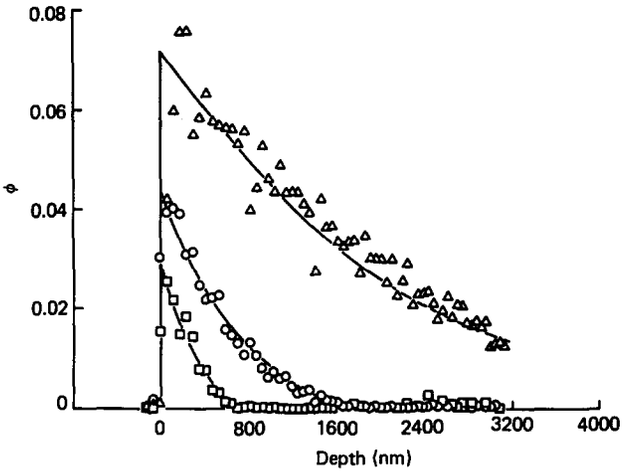

Figure 4 Penetrant volume fraction *versus* depth profiles of iodohexane in polystyrene at $\phi_e \approx 0.083$ and $T = 22.5$°C after exposure times of 1.3×10^4 s (□), 10^5 s (○) and 1.5×10^6 s (△)

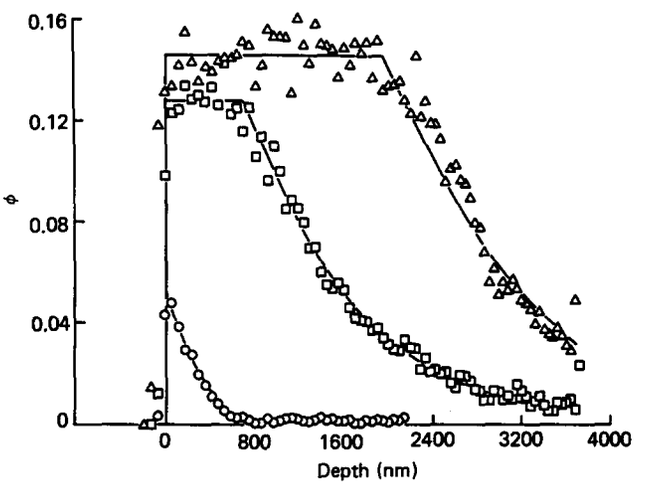

Figure 5 Penetrant volume fraction *versus* depth profiles of iodohexane in polystyrene at $\phi_e = 0.16$ and $T = 22.5$°C after exposure times of 10^4 s (○), 4.1×10^5 s (□) and 7.6×10^5 s (△)

It appears from *Figure 5* that the surface concentration must reach a certain value before Case II diffusion begins. Hence a quantitative representation of the surface swelling kinetics should aid in the understanding of the induction time and its dependence on activity. In addition, a detailed description of the swelling kinetics is necessary to predict the steady-state front velocity[14].

Surface swelling kinetics

The relaxation of the polymer in response to the osmotic pressure may be followed by plotting the surface volume fraction, ϕ_s, as a function of time. Two such plots are shown in *Figures 6* and *7* for $\phi_e = 0.083$ and $\phi_e = 0.16$, respectively. The solid line is the result of numerically integrating equation (9) using the following values of the parameters: $\eta_0 = 8 \times 10^{14}$ N s m^{-2}, $m = 25$ and $\phi_i = 0$ (ref. 13). (The value of η_0 was derived from shear viscosity data of Plazek and O'Rourke (cited in ref. 14) and was converted to an elongational viscosity[26]. The value of

* The aluminium substrates were etched to improve the adhesion of the PS film.

* It was noticed on some of the penetrant volume fraction depth profiles that the penetrant volume fraction at the surface was slightly lower than that approximately 100 nm below the surface. This artefact was attributed to diffusion of penetrant out of the PS film in the 15 s required to transfer the film from the Erlenmeyer flask to the liquid nitrogen.

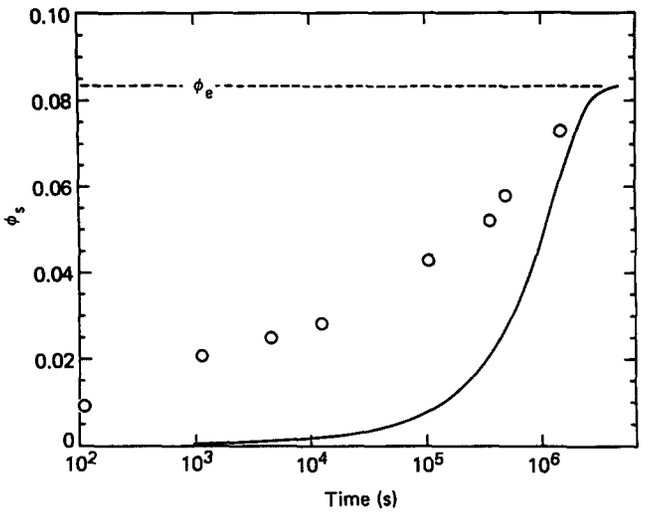

Figure 6 The surface penetrant volume fraction of iodohexane in polystyrene *versus* time for $\phi_e = 0.083$ and $T = 22.5°C$. The solid line is obtained by numerically integrating equation (9) with $m = 25$ and $\eta_0 = 8 \times 10^{14}$ N s m^{-2}

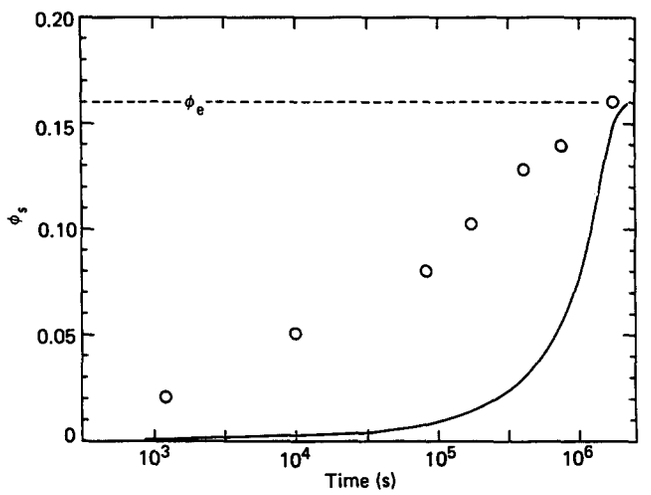

Figure 7 The surface penetrant volume fraction of iodohexane in polystyrene *versus* time for $\phi_e = 0.16$ and $T = 22.5°C$. The solid line is obtained by numerically integrating equation (9) with $m = 25$ and $\eta_0 = 8 \times 10^{14}$ N s m^{-2}

$m = 25$ was chosen to give a good fit to the swelling data at long times and is close to the value assumed by Thomas and Windle[2] for the methanol–PMMA system.) The agreement between the linear viscous swelling model (equation (9)) and experiment is poor. Although the correct order of magnitude for the equilibration time can be predicted with a suitable choice of m, the kinetics of the approach to equilibrium cannot. The initial rate of penetrant volume fraction increase is faster than that predicted by equation (9) whereas the rate at high volume fractions is slower than predicted. The failure of the simple linear viscous model of polymer swelling is not surprising. The osmotic pressures correspond to stresses well above those at which linear viscoelasticity might be expected to hold. Improved agreement between theory and experiment may be obtained by using an expression for viscosity that decreases exponentially with osmotic pressure[13], i.e.

$$\eta = \eta_0 \exp(-m\phi)\exp(-\alpha' P) \qquad (14)$$

where α' is material constant. Substituting equations (14) and (4) into equation (6) changes equation (9) to

$$t = (1/B) \int_{\phi_{fv}}^{\phi} \{\exp(-m\phi)/\ln\Theta\}\Theta^{-\alpha} d\phi \qquad (15)$$

where $\alpha = kT\alpha'/\Omega$. The lower limit of the integral was selected as the volume fraction of interstitial sites ϕ_{fv} ('free volume') that can be occupied by the IOH molecules without polymer chain relaxation. For all further calculations ϕ_{fv} is taken to be approximately equal to 0.02[24].

A simple set of creep experiments was performed to obtain approximate values for α and η_0; these experiments are described in the Appendix. The results of these experiments, $\alpha = 2.05$ and $\eta_0 = 1.9 \times 10^{15}$ N s m^{-2}, were used in the numerical integration of equation (15) with the same value of $m = 25$ as before. The results of this integration for $\phi_e = 0.083$ and 0.16 are compared to the surface volume fraction data in *Figures 8* and *9*, respectively. The agreement between data and theory is now more satisfactory.

Although the swelling kinetics at low activities are in

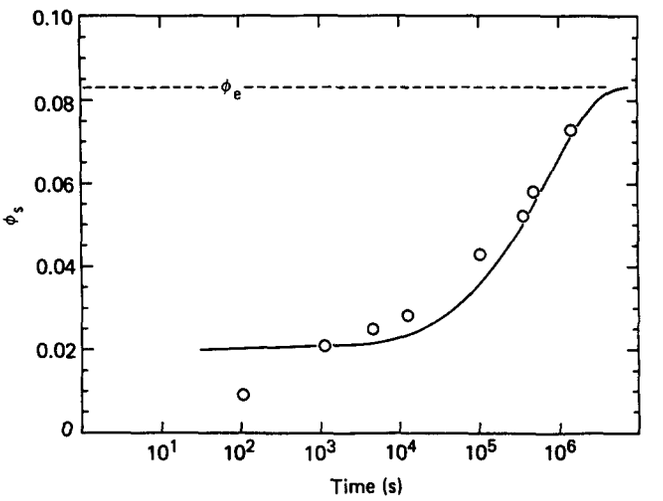

Figure 8 The data is the same as in *Figure 6*. The solid line is obtained by numerically integrating equation (15) with $m = 25$, $\alpha' = 1.22 \times 10^{-7}$ m^2 N^{-1} and $\eta_0 = 1.9 \times 10^{15}$ N s m^{-2}

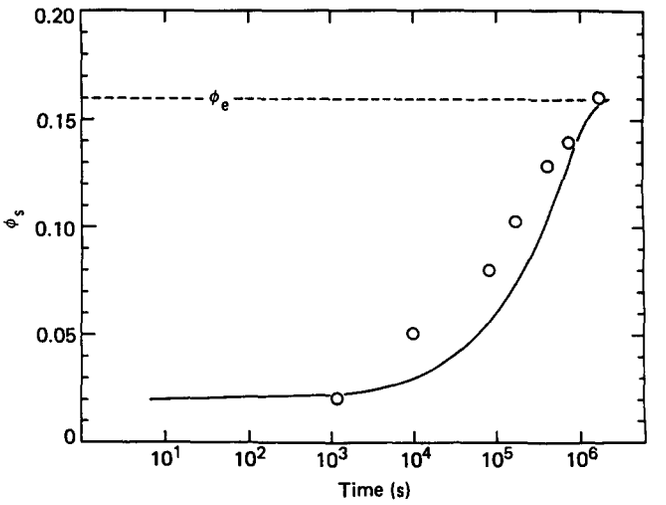

Figure 9 The data is the same as in *Figure 7*. The solid line is obtained by numerically integrating equation (15) with $m = 25$, $\alpha' = 1.22 \times 10^{-7}$ m^2 N^{-1} and $\eta_0 = 1.9 \times 10^{15}$ N s m^{-2}

reasonable accord with the simple nonlinear viscous model (equation (15)), the kinetics at values of ϕ_e greater than 0.2 ($a_e > 0.45$) are not[27]. At these higher activities the osmotic pressure may be large enough to cause yielding in the plasticized polystyrene. If stresses in this regime exist it is unreasonable to assume that the simple nonlinear model can describe the swelling kinetics.

Case II front formation

The preceding data have enabled us to investigate the surface swelling kinetics at different values of ϕ_e. A qualitative discussion of the formation of the Case II front will now be given. At low ϕ_e the IOH volume fraction at the surface increases slowly, accompanied by nearly Fickian diffusion into the bulk PS. When a critical surface volume fraction of penetrant is reached, Case II diffusion begins. In our experiments the critical surface volume fraction of IOH penetrant was approximately equal to 0.1. This amount of penetrant is sufficient to lower the viscosity of the polystyrene and increase the diffusivity of the penetrant to the levels required to create the Case II front.

If ϕ_e is too low, the initial osmotic pressure of the penetrant will be low. The polymer viscosity will remain high and the penetrant diffusivity will remain low even when the swelling nears equilibrium. The combination of these effects will not permit the swelling and diffusion rates required for Case II diffusion front propagation and hence Case II diffusion will never occur. It appears that this situation exists when $\phi_e \leq 0.083$. Thus as ϕ_e is decreased toward the critical value for Case II diffusion, the induction time for Case II diffusion should increase rapidly; below the critical value that time becomes effectively infinite, and quasi-Fickian diffusion only is observed.

CONCLUSIONS

1 The Thomas and Windle model, which was modified to include a pressure-sensitive viscosity, quantitatively describes the surface swelling kinetics of polystyrene exposed to iodohexane at relatively low activities.

2 Case II diffusion begins after a critical surface volume fraction of penetrant ϕ_c is reached. For PS/IOH, $\phi_c \approx 0.1$.

3 Since time is required for the surface volume fraction of penetrant to reach ϕ_c, an induction time for Case II diffusion exists.

4 After the critical surface volume fraction of penetrant is reached and Case II diffusion begins the penetrant volume fraction behind the front slowly approaches its equilibrium value ϕ_e. These swelling kinetics are low even though the diffusion coefficient behind the front is much larger than that in the polymer glass ahead of the front.

ACKNOWLEDGEMENTS

Primary support by the US Army Research Office (Durham) is gratefully acknowledged. We also benefited from the use of the facilities of the Cornell Material Science Center at Cornell, which is funded by the NSF–DMR–MRL program. C. Y. Hui acknowledges the support of the National Science Foundation, through the Cornell Material Science Center. One of us (R.C.L.) received fellowship support from IBM. We greatly appreciate the enthusiastic guidance of Professor J. W. Mayer on all aspects of RBS and we thank Dr R. Ognjanovic for helpful comments on the manuscript.

REFERENCES

1 Scott, J. R. *Trans. Inst. Rubber Industries* 1937, **13**, 109
2 Thomas, N. L. and Windle, A. H. *Polymer* 1982, **23**, 529
3 Thomas, N. L. and Windle, A. H. *Polymer* 1977, **18**, 1195
4 Thomas, N. L. and Windle, A. H. *Polymer* 1978, **19**, 255
5 Thomas, N. L. and Windle, A. H. *Polymer* 1980, **21**, 619
6 Thomas, N. L. and Windle, A. H. *Polymer* 1981, **22**, 627
7 Windle, A. H. in 'Polymer Permeability' (Ed. J. Comyn), Elsevier, 1985, p. 75
8 Alfrey, T. *Chem. Eng. News* 1965, **43**, 64
9 Hopfenberg, H. B., Holley, R. H. and Stannett, V. *Polym. Eng. Sci.* 1969, **9**, 242
10 Holley, R. H., Hopfenberg, H. B. and Stannett, V. *Polym. Eng. Sci.* 1970, **10**, 376
11 Baird, B. R., Hopfenberg, H. B. and Stannett, V. *Polym. Eng. Sci.* 1971, **11**, 274
12 Jacques, C. H. M., Hopfenberg, H. B. and Stannett, V. *Polym. Eng. Sci.* 1973, **13**, 81
13 Hui, C. Y., Wu, K. C., Lasky, R. C. and Kramer, E. J. *J. Appl. Phys.* 1987, **61**, 5129
14 Hui, C. Y., Wu, K. C., Lasky, R. C. and Kramer, E. J. *J. Appl. Phys.* 1987, **61**, 5137
15 Flory, P. J. 'Principles of Polymer Chemistry', Cornell University Press, Ithaca, NY, 1953, Ch. 12
16 Guggenheim, E. A. 'Applications of Statistical Thermodynamics', Clarendon Press, Oxford, 1966, Ch. 7
17 Chu, W. K., Mayer, J. W. and Nicolet, M. A. 'Backscattering Spectrometry', Academic Press, New York, 1978, Ch. 2 and 3
18 Zeigler, J. F. 'The Stopping and Ranges of Ions in Matter', Vol. 4, Pergamon, New York, NY, 1977, Vol. 4
19 Anderson, H. and Ziegler, J. F. 'The Stopping and Ranges of Ions in Matter', Vol. 3, Pergamon, New York, 1977
20 Doolittle, L. R. *Nucl. Instrum. Meth.* 1985, **B9**, 344
21 Doolittle, L. R. *Nucl. Instrum. Meth.* 1986, **B15**, 227
22 Romanelli, J. F., Mayer, J. W. and Kramer, E. J. *J. Polym. Sci., Polym. Phys. Edn.* 1986, **24**, 263
23 Struik, L. C. E. 'Physical Aging of Amorphous Polymers and Other Materials', Elsevier, Amsterdam, 1978, Ch. 1, p. 173
24 Roe, R. J. and Millman, G. M. *Polym. Eng. Sci.* 1983, **23**, 318
25 Mills, P. J., Palmstrøm, C. J. and Kramer, E. J. *J. Mater. Sci.* 1986, **21**, 1479
26 Bird, R. B., Armstrong R. C. and Hassager, O. 'Dynamics of Polymer Liquids', Vol. 1, Wiley, New York, Ch. 7–9
27 Lasky, R. D. *Ph.D. Thesis*, Cornell University, 1986, p. 101

APPENDIX

Determination of material constants in the viscosity relationship

Simple creep experiments were performed to obtain approximate values for the material constants α' and η_0 in the expression for viscosity:

$$\eta = \eta_0 \exp(-m\phi)\exp(-\alpha' P) \qquad \text{(A1)}$$

Polystyrene was compression moulded into dog-bone-shaped samples at a temperature of 225°C. The annealing and ageing parameters of the dog bone samples were the same as those used in the RBS experiments. The creep was monitored with a linear variable differential transformer (LVDT). Tensile stress was applied to the dog-bone-shaped samples by dead weight loading.

It was assumed that the strain rate of the sample was given by

$$\partial\varepsilon/\partial t = \sigma/\eta \qquad \text{(A2)}$$

where ε is the strain, σ is the stress and η is the viscosity.

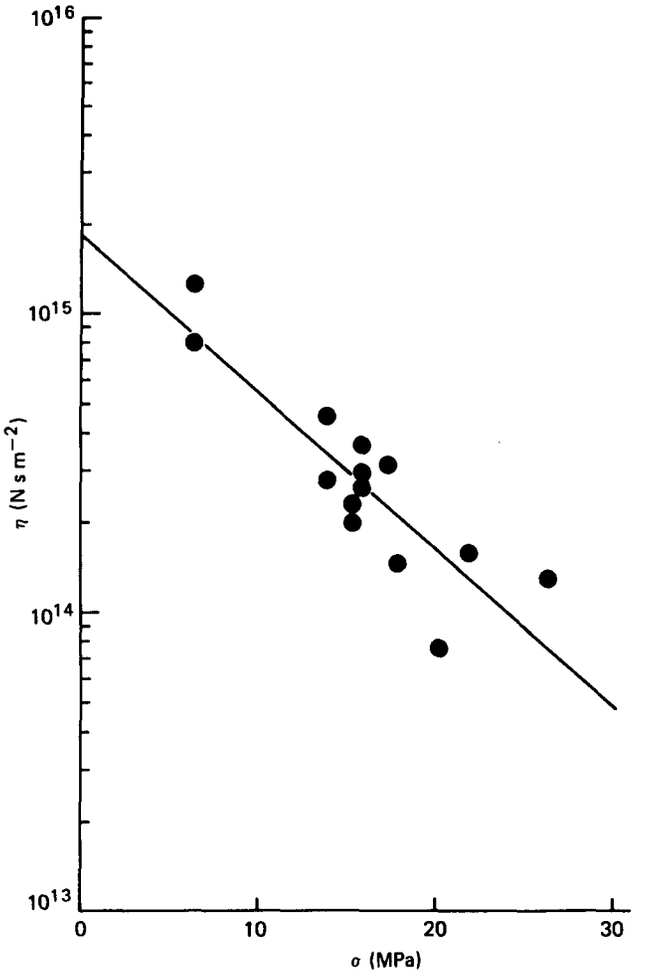

Figure 10 The elongational viscosity of polystyrene *versus* stress at 22.5°C. The line is a least squares linear fit to the data, as discussed in the text

The viscosity η was computed from the slope of the ε *versus* time curve ($\varepsilon(t)$). Since the slope of the $\varepsilon(t)$ curve decreased with t at short times this procedure gives rise to potential ambiguity. However, since the experiments that measured the surface swelling kinetics were usually many hours in length, this early section of the $\varepsilon(t)$ curve was ignored and the slope was not taken until more than 30 min into the creep test. Creep experiments were performed at different stresses and the η values extracted are plotted *versus* stress in *Figure 10*. These data may be represented, over this narrow range of σ, by

$$\eta = \eta_0 \exp(-\alpha' \sigma) \tag{A3}$$

which is the analogue of equation (A1) at $\phi = 0$. Values for η_0 and α' were obtained from these data by least squares analysis, resulting in $\eta_0 = 1.9 \times 10^{15}$ N s m^{-2} and $\alpha' = 1.22 \times 10^{-7}$ m^2 N^{-1} (or $\alpha = 2.05$). The correlation coefficient for this analysis was 0.922 and the 90% confidence limits for η_0 were $\pm 0.44 \times 10^{15}$ N s m^{-2} and for $\alpha' \pm 0.23 \times 10^{-7}$ m^2 N^{-1}.

It is not obvious that the value of α' determined in these creep experiments should be the same as the value in equation (A1). We assume that it is because of the following argument. The glass ahead of the front constrains the swelling of the polymer to be uniaxial and normal to the surface. The value of α' obtained from a tensile creep experiment most closely duplicates the value of α' expected to apply in the constrained swelling experiment.